LANDSCAPE EVOLUTION AFTER THE 2014–2015 LAVA FLOW AT HOLUHRAUN, ICELAND.

L. E. Bonnefoy[1], C. W. Hamilton[1], S. P. Scheidt[1], J. Voigt[2], À. Hoskuldsson[3], I. Jónsdottir[3], and T. Thordarson[3], [1]Lunar and Planetary Laboratory,University of Arizona,Tucson,AZ USA,[2]German Aerospace Center (DLR),Institute of Planetary Research, Germany, [2]Faculty and Institute of Earth Sciences, University of Iceland, Reykjavík, Iceland.

Introduction: The main phase of the Holuhraun eruption lasted from August 31, 2014 to February 27, 2015 and created an 83.5 km^2 lava flow field (Fig. 1). The eruption was preceded by an earthquake swarm, ground fractures, and graben subsidence [1], accompanied by caldera subsidence in the Bárðarbunga central volcano [2], and generated substantial sulfur pollution [3]. This event was the largest magma outpouring (1.1-1.2 km^3 Dense Rock Equivalent; DRE [4]) in an eruption in Iceland since the 1783–1784 Laki event (15 km^3 [5]). The 2014–2015 eruption site had already experienced two eruptive fissures, in 1797AD and 1867AD. All three of these events produced magma that has compositional affinites to the Bárðarbunga system [6], further pointing to it as the source of the magma. Given the proximity of the 2014-15 lava field to the Askja volcano and Vatnajökull ice cap, high-resolution Digital Terrain Models (DTMs) had been obtained prior to the 2014–2015 eruption. Combining this pre-eruption dataset with post-emplacement DTMs allows to compute the lava flow volume and investigate landscape evolution processes associated with the eruption.

Methodology: We assembled different datasets to obtain two DTMs over the 2014–2015 lava flow field, corresponding to before (2013) and after (2015) the lava emplacement.

The pre-emplacement DTM (Fig. 2A) was processed from airborne photogrammetry datasets by Loftmyndir ehf. and was generated by combining datasets and smoothing the seams. The spatial resolution is 5 m/pixel, and error bars in elevation vary from ±0.5 m to ±5 m. We document the variable quality of the pre-eruption DTM, in a figure of merit (Fig. 2B).

The post-emplacement DTM (Fig. 2C) uses a combination of datasets to obtain the best possible quality of data over the whole region. LiDAR data, taken in August 2015 and processed by the Natural Environment Research Council (NERC), has the highest resolution (2 m/pixel). Where LiDAR data was unavailable, we used another photogrammetry DTM provided by Loftmyndir ehf., processed from data taken in August 2015. Where large clouds obscured parts the region of interest, the data was simply interpolated. Where a cloud covered the edge of the flow, contour lines were estimated using ArcGIS' editing tools for every meter using only the orthoimage as reference.

Additionally, we conducted a field campaign in the 2014–2015 Holuhraun lava flow field in the summers of 2015 and 2016, taking high-resolution Unmanned Aerial Vehicle (UAV) observations in several areas shown in Fig. 1 [7,8]. The regions of interest chosen for these high-resolution DTMs are the vent region (region A), lateral flow margin (region B) and hot springs located at the distal margin (region C). Both the pre- and post-emplacement DTMs were georeferenced using Differential-GPS measurements.

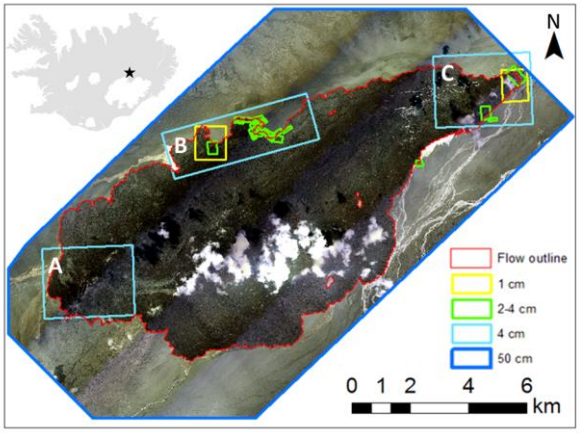

Fig. 1: Resolution and footprints of acquired DTMs over the lava flow. The flow outline is shown for reference. The background orthoimage was created from the 2015 observations by Loftmyndir ehf.. A: Vent region. B: Flow margin. C: Hot springs region. The position of the Holuhraun lava field in Iceland is shown in the top left corner.

Results: A difference map was created between the after and before lava flow field DTMs to show any changes in the topography of the region (Fig. 2E). We note the presence of graben subsidence in the southwest corner of the flow, due to dyke intrusion, as detailed by [1]. From this difference map, we calculate the bulk volume of deposited lava to be $1.46^{+0.04}_{-0.06}$ km^3. This value is consistent with the bulk volume of 1.44 km^3 and DRE volume of 1.1–1.2 km^3 found by [4].

The lava flow occurred over the floodplain of the Vatnajökull ice cap, a rather flat and regularly sloped large area with interweaving riverbeds. The lava naturally flowed downslope, along and around the main riverbeds. The most recent eruption partially covers older flow fields and on the north side it is banked up against the 1924–1929 lava flow field from Askja [9]. Indeed, the presence of the flow field from Askja (Fig. 2A) caused the main river channels from the west of

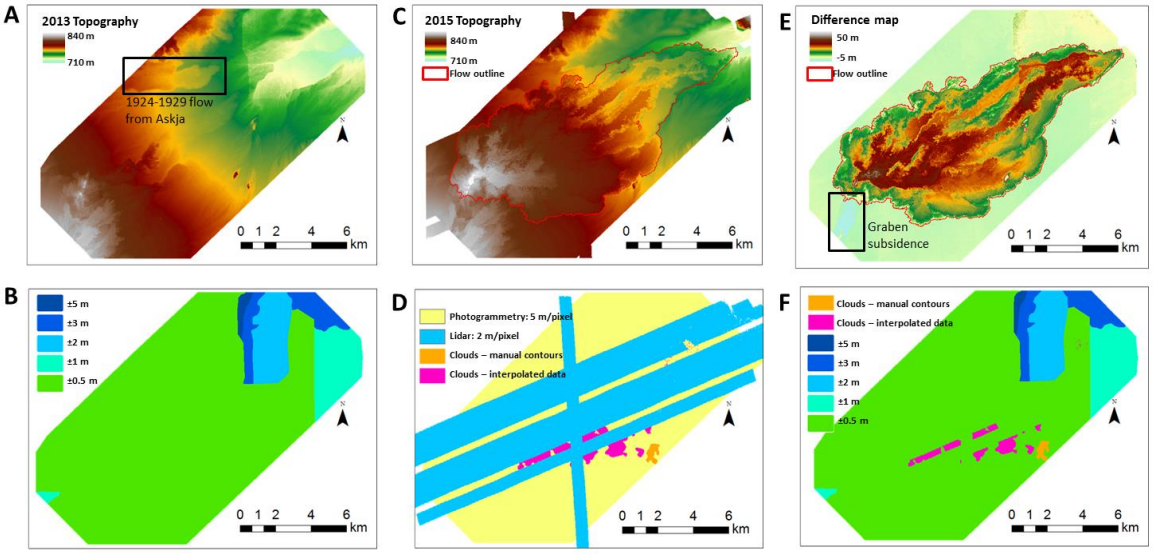

Fig. 2: Topography in the region of interest before and after the 2014–2015 eruption. A. Pre-emplacement topography. The DTM has a spatial resolution of 5 m/pixel. B. Figure of merit for the pre-emplacement topography: error bars in elevation. C. Post-emplacement (2015) topography. D. Figure of merit for 2015 topography. E. Difference map, showing the lava flow and the graben in the Southwest corner. F. Figure of merit for the difference map.

the flood plain to redirect eastward, creating banks as high as 6 m. The northern boundary of the 2014–2015 lava flow field initially followed the river bank, but was later modified by inflation, overlapping the 1924–1929 Askja flow field in places (Fig. 1 region B) [4].

After the end of the deposition of lava in February 2015 and once spring arrived, the meltwater from the Vatnajökull glacier went under and through the lava, thus creating hot springs when exiting. The water increasingly ponded at the entry points into the lava, creating lakes and digging new streambeds (Fig. 1). According to eye-witness accounts by rangers within the Vatnajokull National Park, the lava-dammed lake remained stable until the summer of 2016. On July 15, 2016, a small trickle of water was observed along eastern side of the flow, but was not fully connected to the hot springs until July 21. The main phase of the breach occured on July 22, when glacial water began flowing into the hot springs with large waves pouring through the gap. On July 22 and 23, a huge steam plume was seen rising from the location of the former lake. After the breach, water primarly flowed along the edge of the lava, but observations of water flux through pools in the lava and from the springs located at the distal flow margin imply that some water continued to flow through and beneath the lava. After July 22, glacier riverwater and hot springs water merged in the C region (Fig. 1) producing braided stream branches with a wide range of temperatures.

The floodplain was also a region of active aeolian sand ripples and aeolian mantling of the lava's northern margin. The new material, changed winds, and modified hydrology show strong evidence of how the flow has affected surface processes near the edge of the lava flow. This dataset gives us a unique opportunity to study the dynamics of sediment by both wind and water along the lava flow margins in sand sheets, which can be compared to regions on Mars.

Conclusion: The availability of high-resolution topography both before and after the 2014–2015 fissure eruption at Holuhraun allows us to study the evolution of both hydrological and sedimentary/aeolian processes due to the emplacement of a large lava field. The updated volume of lava deposited during the 2014–2015 eruption is of $1.46^{+0.04}_{-0.06}$ km^3. The interaction of sand sheets, floodplain hydrology, and a fissure eruption is especially reminiscent of Martian processes.

References: [1] Hjartardóttir Á. R. et al. (2016) *Journal of Volcanology and Geothermal Research, 310*, 242-252. [2] Gudmundsson M. T. et al. (2016) *Science, 353*, 6296. [3] Schmidt A. et al. (2015), *Journal of Geophysical Research: Atmospheres, 120*, 9739-9757. [4] Thordarsson T. et al. (2015) *AGU fall meeting*, Abstract #V13D-01. [5] Thordarsson and Self (1993) *Bulletin of Volcanology, 55*, 233-263. [6] Hartley, M. E. et al. (2016) *Bull Volcanol. 78*, 28. [7] Hamilton C. W. (2015) *Eos, 96*. [8] Hamilton C. W. et al. (2015) *GSA Annual Meeting*, Abstract #264973. Poster [9] Hartley, M. E. and Thordarson, T. (*2013) Geochemistry, Geophysics, Geosystems, 14*, 2286—2309.